Physical Sciences - Daytona Beach   College of Arts & Sciences

2-11-2005

Climatology of Short-Period Gravity Waves Observed over Northern Australia during the Darwin Area Wave Experiment (DAWEX) and their Dominant Source Regions

P. -D. Pautet
Utah State University

M. J. Taylor
Utah State University

Alan Z. Liu
Embry Riddle Aeronautical University - Daytona Beach, liuz2@erau.edu

Gary Swenson
University of Illinois at Urbana-Champaign

Follow this and additional works at: https://commons.erau.edu/db-physical-sciences

Part of the Physical Sciences and Mathematics Commons

Scholarly Commons Citation

Climatology of short-period gravity waves observed over northern Australia during the Darwin Area Wave Experiment (DAWEX) and their dominant source regions

P.-D. Pautet and M. J. Taylor

Center for Atmospheric and Space Sciences, Utah State University, Logan, Utah, USA

A. Z. Liu and G. R. Swenson

Department of Electrical and Computer Engineering, University of Illinois, Urbana, Illinois, USA

[1]   The Darwin Area Wave Experiment (DAWEX) was designed to investigate the generation and propagation of gravity waves from intense regions of localized convection that occur regularly over northern Australia (in the vicinity of Darwin) during the premonsoon period. This multinational program was conducted during the austral spring 2001 using a range of coordinated optical, radar, and in situ balloon measurements. As part of this program, all-sky image observations of short-period gravity wave events in the near infrared OH nightglow emission (altitude ~87 km) were made from two well-separated sites in northern Australia: Wyndham (15.5°S, 128.1°E) and Katherine (14.5°S, 132.3°E), over a 10-day period during November 2001. A total of 25 extensive wave events were observed during this period, from which the dominant horizontal wave characteristics were determined to be: wavelength 25–35 km and observed phase speed 27–75 m/s, yielding observed periods from 7 to 14 min, consistent with previous measurements at other low-latitude sites. A key finding of this study was a marked anisotropy in the wave propagation headings, with over 3/4 of the events exhibiting a strong southward component of motion and a clear preference for wave progression over the azimuthal range SE to SSW. Although this range encompasses gravity waves originating locally from the Darwin area, the majority of the wave events exhibited propagation headings consistent with more distant sources located to the north and northwest of Australia. Assuming deep convection was the dominant mechanism for the waves, the strong asymmetry in their velocity distribution appears to result from a combination of nonuniformity in the geographic occurrence of thunderstorms coupled together with significant wind filtering effects at the source altitude and within the middle atmosphere. These results are consistent with long-range, short-period wave propagation (most probably in the form of ducted waves) possibly from intense convective regions located ~1000 km to the north over the Indonesian Island chain.

1.   Introduction

[2]   There is now little doubt that gravity waves play a key role in defining the thermal structure and large-scale circulation of the mesosphere and lower thermosphere (MLT) region (altitude ~60–100 km). Although thermal tides and planetary waves dominate the instantaneous motion fields at these heights (due to their large horizontal and vertical amplitudes), by far the largest systematic influence on the MLT region results from much smaller scale, freely propagating, gravity waves that can transport large amounts of momentum from sources in the lower atmosphere up into the MLT region. In particular, vertical transport of horizontal momentum by gravity waves is thought to play a crucial role in defining the global-scale circulation throughout the middle atmosphere region. [e.g., *Lindzen*, 1981; *Holton*, 1983; *Garcia and Solomon*, 1985; *Hamilton*, 1996; *Alexander and Holton*, 1997; *Fritts and Alexander*, 2003].

[3]   A wealth of potential gravity wave sources exists within the tropospheric region, the distributions of which are expected to vary significantly with both season and geographic latitude. Of considerable importance at low and equatorial latitudes is the role of strong convection in forcing vertically propagating short-period (<1 hour) gravity waves. Numerous modeling and theoretical studies indicate

that convectively generated gravity waves, which exhibit relatively large vertical wavelengths (> several km), can play a major role in defining the flow of momentum into the MLT region [e.g., *Alexander et al.*, 1995, 2004; *Holton and Alexander*, 1999; *Horinouchi et al.*, 2002; *Beres et al.*, 2004]. In particular, previous coordinated investigations of MLT dynamics, such as the ALOHA-90 and 93 campaigns, have established copious short-period wave activity over the central Pacific Ocean [e.g., *Taylor and Hill*, 1991; *Swenson et al.*, 1995; *Taylor et al.*, 1995a], much of which is expected to be generated by convective forcing. Furthermore, these observations have demonstrated the importance of coincident, multi-instrument measurements for studying the effects of gravity waves on the MLT region. To this end, the Darwin Area Wave Experiment (DAWEX) was conceived to investigate the generation and propagation of gravity waves from a well-defined convective source region into the upper reaches of the MLT where they can be detected readily by their signatures in the naturally occurring nightglow emissions (altitudes ∼80–100 km) [e.g., *Moreels and Herse*, 1977; *Taylor and Hill*, 1991; *Swenson and Mende*, 1994; *Smith et al.*, 2000; *Medeiros et al.*, 2003; *Nakamura et al.*, 2003].

[4] The DAWEX campaign took place in northern Australia, throughout the austral spring from mid-October to mid-December 2001. During this period the local convective activity changed in a systematic manner from premonsoon, with little convection, to summer monsoon conditions with an associated dramatic increase in the intensity and geographical extent of deep tropical storm convection [*Hamilton and Vincent*, 2000; *Hamilton et al.*, 2004]. In particular, the Tiwi Islands (Melville and Bathurst Islands) located just off the coast to the north of Darwin are home to an unusual diurnal convection pattern that occurs during the late premonsoon period and gives rise to an intense, confined region of convection (with vertical updrafts as strong as 40 m/s), that frequently reaches tropopause altitudes (∼20 km) by midafternoon [e.g., *Keenan and Carbone*, 1992; *Carbone et al.*, 2000]. This storm is driven by local sea breeze circulation and is so regular that it is colloquially called "Hector" by the local inhabitants. The goal of the DAWEX experiment was to investigate, through observations and realistic modeling, the connection between convectively forced gravity waves from Hector (and other intense storm activity) that occurred in the vicinity of Darwin at that time and the gravity wave field observed subsequently at MLT heights.

[5] A number of different instruments were deployed for this program, centered mainly on northern Australia, but extending to Adelaide in southern Australia. This paper focuses on measurements obtained using two all-sky CCD cameras that were capable of imaging short-period gravity wave signatures as they propagated through the nightglow emission layers. The observations were made from two well-separated sites at Katherine, Northern Territory and at Wyndham, Western Australia, to determine the general characteristics of the nighttime mesospheric gravity wave activity and to identify their dominant directions of motion. In this paper, the data have been used to determine the regional climatology of the wave events observed during the late premonsoon period in 2001, and to perform an initial investigation of the dominant source regions. Surprisingly,

the data suggest more distant sources for the majority of the observed wave events rather than regional convective activity over the Darwin area.

2. Planning and Instrumentation

[6] The DAWEX campaign was organized into three intensive observational periods (IOPs). The first IOP was conducted from 13 to 18 October, prior to the anticipated onset of deep convection over the Darwin area/Tiwi Islands. The second IOP took place during the new moon period 15–20 November and constituted the main measurement period for the campaign. During this interval, intense "Hector-type" thunderstorms occurred over the Tiwi Islands every afternoon, some reaching 18–20 km in altitude. These isolated storms were often followed by strong squall-line activity in the general Darwin area. The third IOP was conducted from 11 to 16 December during the early stages of the summer monsoon period. Many strong thunderstorms were also generated during this interval, primarily in association with intense squall line activity over much of the "top end" of northern Australia, but no further regular-type (Hector) storms were observed over the Tiwi Islands.

[7] A broad range of instruments were deployed during the DAWEX campaign: in situ balloon measurements to investigate convective forcing over the Tiwi Islands [*Tsuda et al.*, 2004], radar measurements to study the prevailing tropospheric and middle atmospheric wind fields [*Vincent et al.*, 2004], and airglow image measurements to investigate the mesospheric response to strong regional convective forcing presented herein and also in the studies of *Hecht et al.* [2004] and *Suzuki et al.* [2004]. Further details on the campaign measurements are given in the work of *Hamilton et al.* [2004].

[8] To measure the gravity wave signatures at MLT heights, coordinated observations were obtained using an array of five nightglow imaging systems; four from institutions in the USA and one from Japan. The instruments were deployed at key sites, spanning the Australian continent from Darwin in the north (12.5°S) to Adelaide in the far south (34.5°S). Table 1 lists the coordinates of these optical sites and their approximate range from the Tiwi Islands/Darwin area. For continuity, each imager was filtered to observe the near infrared OH nightglow emission (∼700–900 nm), which originates from a well-defined layer of half-width ∼8 km, centered at a mean altitude of ∼87 km [e.g., *Baker and Stair*, 1988]. This is the most intense emission in the night sky and has been used on numerous prior occasions to investigate the properties of short-period gravity waves at low, middle and high latitudes [e.g., *Swenson and Mende*, 1994; *Taylor and Henriksen*, 1989; *Taylor et al.*, 1995a, 1997; *Wu and Killeen*, 1996; *Walterscheid et al.*, 1999; *Smith et al.*, 2000; *Hecht et al.*, 2001; *Ejiri et al.*, 2003; *Medeiros et al.*, 2003; *Nakamura et al.*, 1999, 2003].

[9] The image data provided direct information on the occurrence and propagation characteristics of short-period mesospheric wave events of vertical wavelength significantly larger than the OH emission layer thickness ($\lambda_z > \sim 10$ km) [*Swenson and Gardner*, 1998], and over an exceptionally large latitudinal range during this period. In this paper, we utilize data from two all-sky cameras strate-

Table 1. DAWEX Optical Site Information and Distances to the Tiwi Islands

Site	Coordinates	Emissions	Institution	Range to Tiwi Islands, km
Darwin	12.5°S, 130.9°E	OH, OI	University of Nagoya	130
Katherine	14.5°S, 132.3°E	OH	University of Illinois	395
Wyndham	15.5°S, 128.1°E	OH, OI	Utah State University	525
Alice Springs	23.4°S, 133.5°E	OH, O_2	Aerospace Corp	1370
Adelaide	34.4°S, 138.3°E	OH, O_2	Aerospace Corp	2700

gically sited at Wyndham (15.5°S, 128.1°E) and Katherine (14.5°S, 132.3°E), to investigate the occurrence and properties of mesospheric gravity waves in moderately close proximity to the expected convection over the Darwin area. Unfortunately, no data were obtained during IOP 2 and 3 by the Japanese all-sky imager located at Darwin, due to intense storm activity. However, subsequent measurements have been used by *Suzuki et al.* [2004] to investigate gravity wave activity over northern Australia during other seasons. In addition to these data, infrared brightness temperature images recorded by the Japanese Geostationary Meteorological Satellite (GMS) have been used to help identify the main regions of strong convective activity during the campaign.

[10] Figure 1 shows a map of northern Australia indicating the location of the University of Illinois (UI) imager at Katherine, approximately 400 km to the ~SSE (azimuth ~150°N) of the Tiwi Islands, and the Utah State University (USU) imager, sited at Wyndham about 525 km to the ~SW (azimuth ~210°N). The shaded circular areas (300 km radius) indicate the effective field of view of each instrument at ~90 km altitude projected onto the Earth's surface. These two sites are separated by ~465 km to help provide discriminating information on the observed propagation azimuths of gravity waves originating from the expected localized source regions in the vicinity of Darwin. Both imagers were fitted with an all-sky lens (providing a 180° field of view) and a broadband near infrared (NIR) filter (750–930 nm with a notch at 865 nm to suppress contributions from the $O_2(0,1)$ band emission which originates at a slightly higher altitude). Several OH bands occur within this spectral range, the most prominent of which are the OH (9,4), (5,1), (6,2) and (7,3) bands [e.g., *Broadfoot and Kendall*, 1968].

[11] The UI imager was installed at Katherine airport in late October and obtained data during the IOP 2 and 3. This instrument utilized an Apogee camera fitted with a 1024 × 1024 front illuminated CCD array. Sequential images of the OH emission structure were obtained using a 90 sec exposure with a cadence of ~107 sec. To increase the signal-to-noise ratio of the data set, each digital image was binned on chip to 512 × 512 pixels, providing a zenith spatial resolution of ~0.6 km. Further details of this imaging system and its capabilities are given by *Rezaul and Swenson* [1999].

[12] The USU imaging system was equipped with an all-sky telecentric lens and a computer-controlled filter wheel, providing an additional capability to sequentially observe the broadband OH emission and several fainter nightglow emission layers. The $O_2(0,1)$ band and the OI (557.7 nm) emission line, which originate at higher mean altitudes in the upper mesosphere at ~94 km and ~96 km, respectively, were also observed. This imager utilized a Photometrics

CH250 camera fitted with a 1024 × 1024 back thinned CCD array. As with the UI camera, the data were 2 × 2 binned on chip to 512 by 512 pixels providing a similar zenith spatial resolution. Exposure times were 15 sec for the OH data and 90 sec each for the fainter O_2 (0,1) and OI (557.7 nm) data, resulting in a cycle time of ~4 min. However, the high humidity conditions often limited the operation of the CCD detector to −25°C, significantly below its nominal operating temperature of −40°C. The Wyndham measurements therefore focused on observing the NIR OH and the OI (557.7 nm) nightglow emissions (cadence time ~2 min), with occasional O_2 measurements. The USU imager was installed in an ionosonde trailer at Wyndham airport in early November and operated from 12 to 23 November 2001, encompassing IOP 2. Further details of this imaging system and the filter specifications are given in the work of *Taylor et al.* [1995a].

3. Observations and Analysis

[13] Figure 2 shows two example all-sky images of short-period gravity wave structures recorded in the OH emission from Wyndham. Initially the seeing conditions at this site were severely hampered by nearby bush fires, however, on 14 November, local thunderstorm activity washed out much of the smoke and aerosols, permitting detailed observations to subsequently be made. Figure 2a shows an example of a coherent wave pattern imaged on the night of 16/17 November (UT day 320) at 1109 UT. The waves
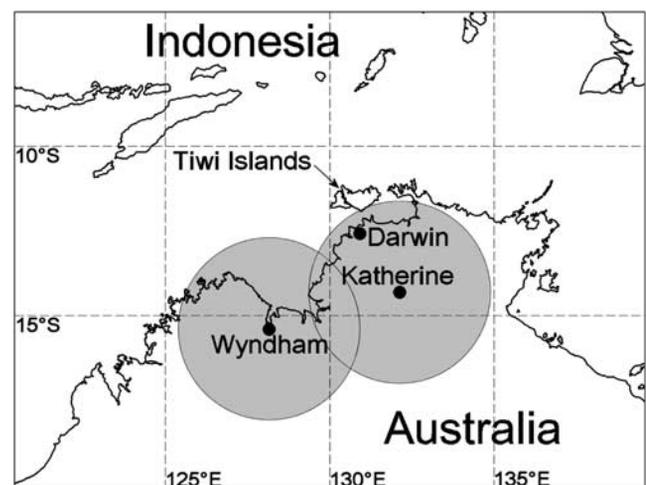
Figure 1. Map showing the locations of the all-sky nightglow imagers operated at Wyndham and Katherine for the DAWEX Campaign. The shaded areas indicate a 300 km radius field of view for each imager at the OH emission altitude.
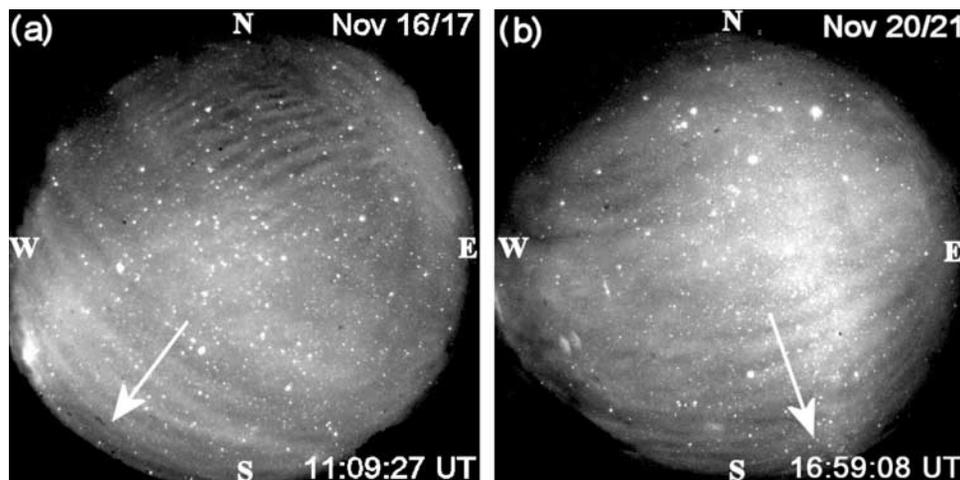
Figure 2. Two images showing short period gravity wave structure in the OH nightglow emission recorded from Wyndham, Western Australia on (a) 16/17 November 2001 and (b) 20/21 November 2001. The white arrows indicate the direction of motion of the dominant wave patterns.

are evident primarily in the lower half of the image and appear to extend from horizon to horizon (observed duration ~2.4 hours). The arrow indicates the direction of propagation of the waves toward the ~SSW. This type of wave pattern is typical of the gravity wave "band" events reported in the literature in association with freely propagating (or ducted) short-period gravity waves observed at low and midlatitudes [e.g., *Taylor et al.*, 1995a; *Isler et al.*, 1997; *Nakamura et al.*, 1999; *Swenson et al.*, 1999; *Walterscheid et al.*, 1999; *Smith et al.*, 2000; *Hecht et al.*, 2001; *Medeiros et al.*, 2003].

[14] In addition to this wave event, a much smaller set of "ripple-like" waves is evident in the upper part of Figure 2a. These events are short-lived (few 10s min) and arise mainly due to localized regions of convective or shear instabilities, generated in situ at mesospheric heights [e.g., *Peterson*, 1979; *Taylor and Hapgood*, 1990; *Fritts et al.*, 1993, 1994; *Hecht et al.*, 1997]. In general, ripple events are not thought to provide direct information on freely propagating gravity waves originating from tropospheric disturbances (see review by *Hecht* [2004]). However, recent three-dimensional modeling studies by *Horinouchi et al.* [2002] suggest that some ripple-like events may be the signatures of larger-scale propagating events breaking in the vicinity of the MLT region. Figure 2b shows a similar-type OH band event (to that present in Figure 2a) recorded on 20/21 November (day 323) at 1659 UT. On this occasion the wave pattern was observed for ~4.5 hours as it progressed overhead at Wyndham on a ~SSE heading (indicated by the arrow). As will be shown later, the overwhelming majority of the wave events observed from Wyndham and Katherine during the DAWEX campaign exhibited a marked preference for southward wave progression.

[15] Figure 3 depicts relative intensity maps derived from the two gravity wave events imaged in Figure 2, following standard airglow image processing. Each figure shows a projection of the wave pattern (as seen from above) onto a rectangular geographical grid of dimensions 300 × 300 km, for an assumed OH emission altitude of 87 km. The data were first calibrated using the known star background to determine accurately the camera orientation and pixel scale
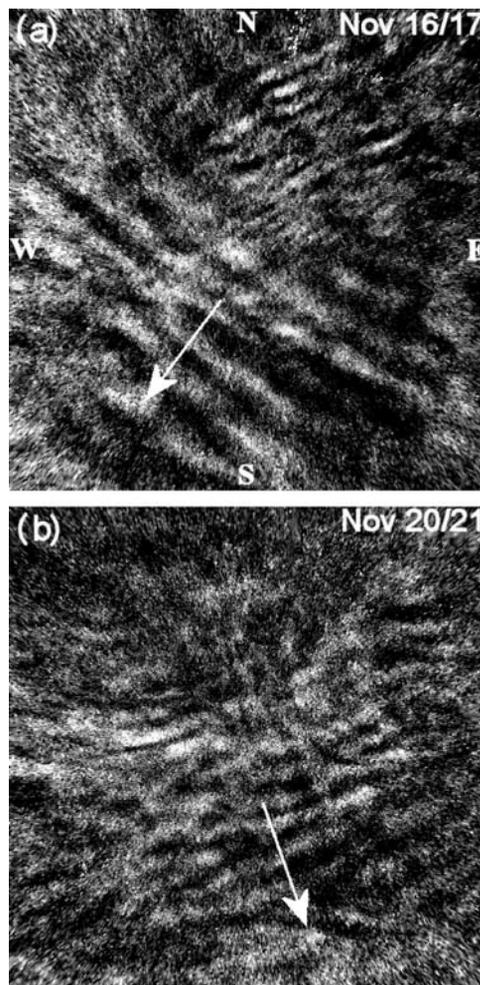
Figure 3. Intensity maps showing the wave structure evident in Figures 2a and 2b projected onto a 300 × 300 km square grid at the Earth's surface. In each example the contrast of the data has been enhanced by subtracting two adjacent images.
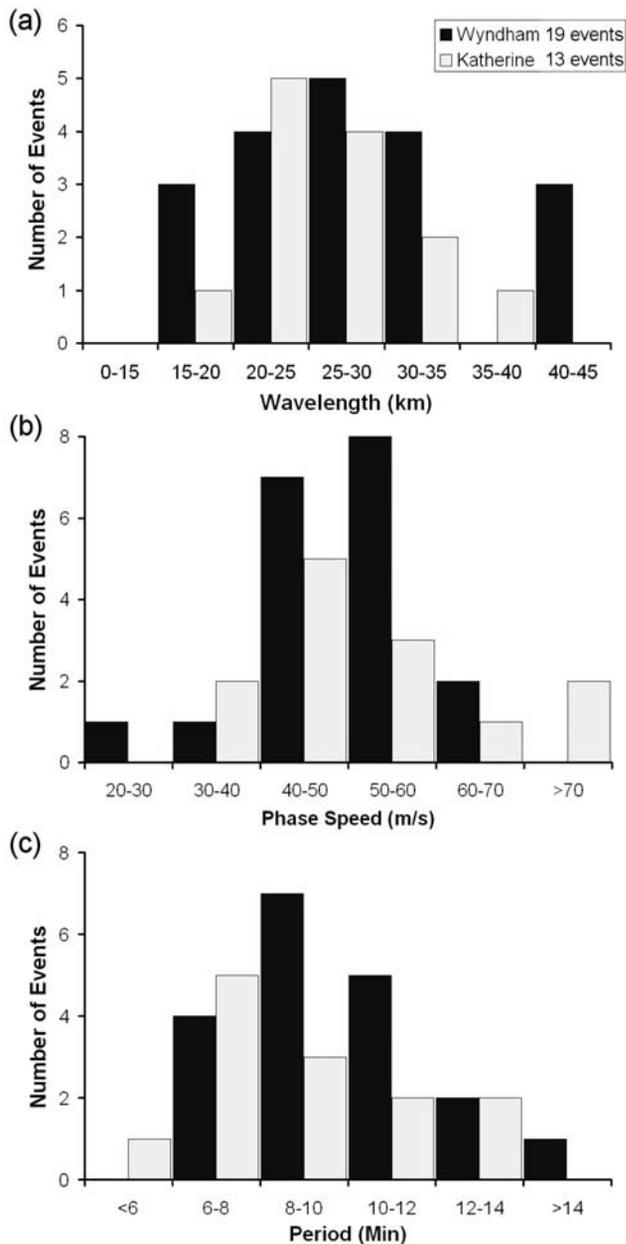
Figure 4. Histogram plots showing: (a) the distribution of horizontal wavelengths for the Wyndham (shaded) and Katherine (light) wave data, (b) the observed phase speed of the waves, and (c) their apparent periodicities. The Wyndham data were recorded during November (IOP 2), while the Katherine data include the November and December periods (IOP 2 and 3).

size, then processed to remove stars and "unwarped" to correct for the all-sky lens format [e.g., *Garcia et al.*, 1997; *Pautet and Moreels*, 2002]. The relatively low contrast (<5%) of much of the wave data recorded at Wyndham and Katherine was due mainly to the low altitude of the sites and to the enhanced level of aerosol scattering that prevailed during the campaign. To help compensate for this problem, the image data have been further processed by subtracting two adjacent images. This technique, termed "difference imaging," has been used by several researchers to enhance the contrast of faint wave structures [e.g., *Swenson and*

Mende, 1994; *Nakamura et al.*, 2003]. The horizontal parameters of each wave event and propagation headings were then determined using well-developed tools employing Fourier transform techniques [e.g., *Taylor and Garcia*, 1995; *Gardner et al.*, 1996; *Garcia et al.*, 1997; *Coble et al.*, 1998] and video motion analysis techniques.

[16] Analysis of Figure 3a reveals a quasi-monochromatic wave pattern exhibiting a horizontal wavelength $\lambda_h = 22$ km, an observed horizontal phase speed $\nu_h = 46$ m/s (as measured with respect to the ground), and an observed period $\tau = 8.0$ min. On this occasion, the gravity waves were seen to progress uniformly toward the ∼SSW at an azimuth of 210°. In contrast, Figure 3b shows a more complex wave pattern with dominant characteristics ($\lambda_h = 16$ km, $\nu_h = 27$ m/s, $\tau = 9.9$ min) that exhibited a somewhat lower phase speed as it propagated toward the ∼SSE. This direction of motion is quite dissimilar to that evident in Figure 3a possibly suggesting different source regions for these two wave events (see discussion).

4. Results

[17] Figure 4 presents a statistical summary of the Wyndham and Katherine gravity wave data. At Wyndham, a total of 28 distinct wave events were recorded during a 10 night period spanning IOP 2. Nine of the events were transient, ripple-type wave patterns that exhibited short horizontal wavelengths (<15 km), and are not considered further in this analysis of freely propagating (and/or ducted) short-period gravity wave events.

[18] The histogram plot of Figure 4a shows the number of band-type wave events imaged as a function of their horizontal wavelength. The black columns indicate the Wyndham data (19 events) while the light-shaded columns show the cumulative Katherine data (13 events) for IOPs 2 and 3. (Note the reduced number of sightings at Katherine was most probably due to more frequent cloud cover associated with its closer proximity to the Darwin area convection.) In each case, the observed range in wavelengths ∼15–50 km is typical for small-scale, short-period gravity waves observed at other low-latitude sites [e.g., *Nakamura et al.*, 2003; *Medeiros et al.*, 2003] and recently from the Darwin area at other times of the year [*Suzuki et al.*, 2004]. Moreover, both data sets show very similar preferences for waves of horizontal scales ∼25–35 km. The average wavelength for the Wyndham data was 28.5 km and 26.1 km for Katherine.

[19] Figure 4b plots the observed wave phase speeds as a function of their occurrence rate. The measured range was 27–74 m/s with a clear preference (72%) for phase speeds ranging from ∼40 to ∼60 m/s. Again, these data compare favorably with previous low-latitude measurements, but the mean of the observed wave speeds (∼50 m/s for both data sets), is significantly higher than many of the midlatitude events reported in the literature [e.g., *Taylor et al.*, 1995b; *Nakamura et al.*, 1999; *Smith et al.*, 2000]. Figure 4c plots the apparent period of the waves computed from the horizontal wavelength and phase speed data. Owing to their somewhat higher observed phase speeds, the distribution of the apparent periods was limited to ∼7 to 14 min with a peak around 8–10 min. The average period for Wyndham was 9.6 min and 8.6 min for Katherine.
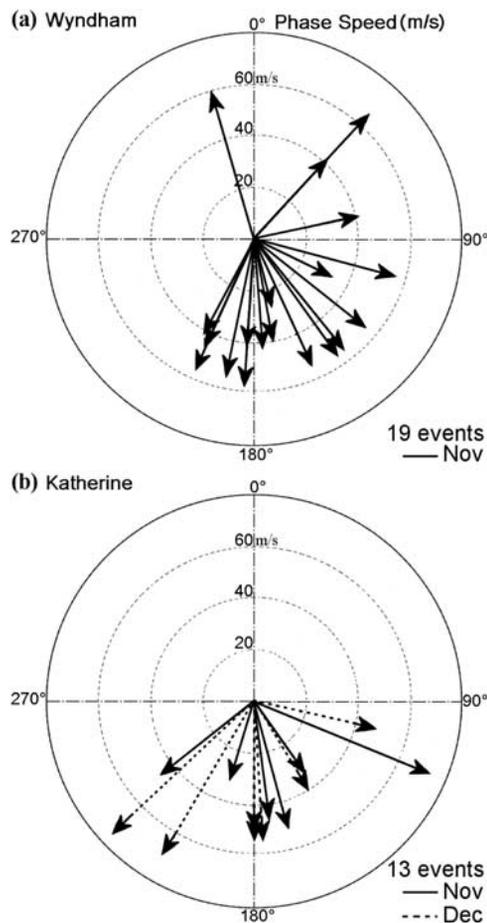
Figure 5. Azimuthal plots showing the distribution of observed wave phase speeds (32 events) as a function of their propagation headings for (a) Wyndham data (IOP 2) and (b) Katherine (IOP 2 and 3). All but four events exhibited a southward component of motion.

[20] Figure 5 plots the azimuthal distribution of the wave events versus their observed phase speed. The length of each arrow indicates the magnitude of the phase speed while the orientation gives its direction of motion to within ±5° as measured clockwise from north. The data from Wyndham (Figure 5a) show a strong preference for southward wave progression with only 4 of the 19 events exhibiting any northward component of motion. In particular, the waves show a clear tendency for progression toward the SE-SSW sector. The Katherine data (Figure 5b) reveal a similar situation with all 13 wave events exhibiting a southward component of motion. In this plot, the wave vectors have been separated into their IOP 2 (solid arrows) and IOP 3 (dashed arrows) observing periods to investigate any preferences in their propagation headings, possibly in association with enhanced convection over the Darwin area. However, both periods show essentially the same broad angular range for wave progression extending from the ∼SE to the ∼SW.

[21] Tables 2 and 3 summarize the measured wave parameters for the band-type events imaged at both sites during the campaign. To distinguish between them, each event is designated by a number (1–19) for Wyndham and a letter (A–M) for the Katherine data. The typical uncertainties in the measurements for both data sets were: horizontal wavelength ±3 km, phase speed ±5 m/s and observed period ±2 min. These values were determined separately for each event using multiple measurements of the wave pattern over a ∼30 min interval of time. This procedure was then repeated approximately every half hour for the duration of the event, and the average value for the horizontal wavelength and observed phase speed computed. Owing to the similar characteristics of the wave data, measurements of individual events yielded comparable uncertainties in their wavelengths and phase speeds, and the errors quoted in the tables represent our best estimate of their mean values.

[22] Each event is described by its measured wave parameters which, coupled together with its observed horizontal direction of motion and time of observation, provides a unique characterization. However, sometimes

Table 2. Summary of Gravity Wave Parameters for the 19 Events Observed From Wyndham During the IOP 2

Date	Day Number	Event	Start, UT	Duration, hours	λ_h (±3 km)	υ_h (±5 m/s)	τ (±2 min)	θ (±5°)
15/16 Nov.	319	1	1044	0.17	25	42	10	185
		2	1818	1.20	18	43	7	175
16/17 Nov.	320	3[a]	1048	2.19	22	46	8	210
		4	1307	1.04	42	65	10.8	45
		5[a]	1607	1.37	17	41	7	215
		6	1847	1.05	30	58	8.6	110
17/18 Nov.	321	7[a]	1032	6.30	30	56	8.9	210
		8	1133	6.05	29	57	8.5	185
		9	1855	0.51	24	55	7.3	155
18/19 Nov.	322	10	1155	2.59	21	40	8.8	170
		11	1738	0.35	44	60	12.2	340
		12	1815	1.39	34	55	10.3	140
20/21 Nov.	323	13	1458	4.30	16	27	9.9	180–150
		14	1931	0.22	45	52	14.4	130
21/22 Nov.	324	15	1516	4.24	33	42	13.1	45
		16	1516	3.56	29	57	8.5	150
		17	1915	0.16	32	54	9.9	195
22/23 Nov.	325	18	1528	0.26	29	42	11.5	75
		19	1715	2.33	22	33	11.1	125

[a]Events consistent with wave origination from the Darwin area.

Table 3. Summary of the Gravity Wave Parameters for the 13 Events Observed From Katherine During IOP 2 and 3

Date	Day Number	Event	Start, UT	Duration, hours	λh (± 3 km)	υh (± 5 m/s)	τ (± 2 min)	θ ($\pm 5°$)
16/17 Nov.	320	A	1240	0.35	31	74	7	125
17/18 Nov.	321	B[a]	1334	1.03	28	45	10.4	170
		C	1352	0.39	20	48	6.9	245
		D[a]	1646	1.25	24	51	7.8	160
18/19 Nov.	322	E	1640	1.13	24	32	12.5	200
19/20 Nov.	323	F	1609	1.22	22	34	10.8	140
15/16 Dec.	349	G	1729	1.19	39	75	8.7	225
		H	1744	1.57	32	40	13.3	145
18/19 Dec.	352	I	1628	2.25	27	48	9.4	180
19/20 Dec.	353	J	1041	7.27	26	52	8.3	175
		K	1046	1.40	22	48	7.6	110
20/21 Dec.	354	L	1530	1.06	28	68	6.9	215
		M	1810	1.06	18	53	5.7	180

[a]Events consistent with wave origination from the Darwin area.

similar-type wave events were observed on the same night but separated well in time. Events 3 and 5 recorded on 16/17 November (Table 2) are good examples of this situation. Event 3 was observed early in the night (around 1100 UT) while event 5 was detected about 5 hours later, around ~1600 UT. Within our measurement uncertainties these two events have the same characteristics and are indistinguishable. However, on this occasion the sky was predominantly clear throughout the night and the OH data plainly show two distinct periods of gravity wave activity associated with these two events. A similar situation occurred on the previous night (15/16 November) for events 1 and 2. The characteristics of these two events are also near identical; event 1 was observed early in the night while event 2 was measured several hours later, toward dawn. However, on this occasion the apparent duration of both events was limited significantly by clouds during the period ~1100 to 1815 UT. Without further information, we have treated these observations as two separate events due to the large time interval (over 7 hours) between them.

[23] Examination of the Katherine data (Table 3) shows a similar situation occurred on 17/18 November (events B and D) which exhibited near identical wave characteristics that were also similar in magnitude, within the measurement uncertainties, to those observed from Wyndham (event 7). As far as we can tell, this is the only wave event that was common to both data sets. This said, the azimuths of these two wave motions were quite different (Katherine ~170° and Wyndham ~210°). However, due to the large (~465 km) separation of the two camera sites (see Figure 1) the observed wave azimuths are nevertheless consistent with wave generation from a common source localized in the general Darwin area. We note here that on this occasion strong convective activity (including Hector) developed in this area during the afternoon and evening period, and this gravity wave event is indicated by an asterisk in the Tables 2 and 3. Other events whose wave azimuths are also well-aligned with a potential convective source over the Tiwi Islands/Darwin area are marked by asterisks in the tables.

[24] Finally, the fact that only one wave event during the IOP 2 appears common to both data sets may seem somewhat surprising, especially given the expected large spatial extent of the band-type wave events [e.g., *Taylor et al.*, 1997]. However, examination of Tables 2 and 3 shows that significant temporal overlap of the two data sets was

obtained on only three occasions during the 10 nights of joint operations at Wyndham and Katherine. This result reflects the difficulty in obtaining coordinated measurements from these two sites due to variable weather conditions accompanying the strong regional convection.

5. Discussion

[25] The DAWEX campaign provided an important opportunity to investigate short-period gravity wave characteristics and dynamics in moderate proximity to expected intense thunderstorm convection over northern Australia. In particular, the data from Wyndham and Katherine indicate significant short-period gravity wave activity during IOP 2 (and 3), when strong convection was present to the north of these sites (no image data were obtained during IOP 1).

[26] The dominant wave motions comprised extensive band-type patterns with occasional, small-scale ripple events. The spatial characteristics of these two types of wave motions are very similar to gravity wave reported in the literature from other latitudes and seasons. In contrast, the distribution of observed horizontal phase speeds was broad, ranging from ~27 to 75 m/s, and exhibited a mean value (~50 m/s) that is significantly larger than similar-type wave studies performed at middle and high latitudes [e.g., *Taylor and Henriksen*, 1989; *Taylor et al.*, 1995a; *Nakamura et al.*, 1999]. However, our DAWEX observations are consistent with other measurements at low and equatorial latitudes [e.g., *Taylor et al.*, 1997, *Nakamura et al.*, 2003; *Medeiros et al.*, 2004; *Suzuki et al.*, 2004], who also reported waves which exhibit peak distributions around 50–60 m/s, or larger. This results in a much narrower range for the apparent wave periods (typically <15 min), compared with observed periodicities up to 30 min (or more) at higher latitudes.

[27] This emerging result may be due to differences in the depth of the convective regions at middle and equatorial latitudes or possibly to the effects of strong horizontal winds near the top of the evolving storm. For example, *Holton et al.* [2002] and *Beres et al.* [2004] have modeled the spectrum of gravity waves above a convective source based on latent heating. Their results show that the dominant vertical wavelength of short-period gravity waves generated by this type of source is expected to depend on the depth of
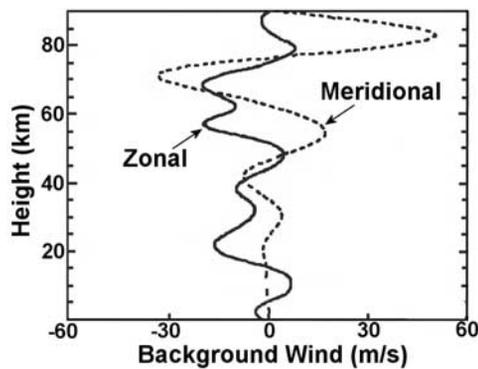
Figure 6. Plot of the zonal and meridional wind components representative for the IOP 2 at 1430 UT (derived from *Hamilton et al.* [2004, Figures 5 and 6]).

the convective/heating region. Furthermore, the observed wave phase speeds are also expected to be proportional to vertical wavelength (through the gravity wave dispersion relationship) and hence to the heating depth. Thus deeper heating associated with more intense convection could excite waves with higher horizontal phase speeds. Tropical storms, which are usually much more vigorous than their midlatitude counterparts and can extend to higher tropopause altitudes, would therefore be expected to generate waves with higher observed horizontal phase speeds. Furthermore, the modeling results of *Beres et al.* [2004] and *Alexander et al.* [2004] show that strong upper tropospheric winds can introduce significant asymmetry in the magnitude and direction of the waves generated by deep convection. As tropospheric winds are, on average, stronger at midlatitudes than at low latitudes this may also affect the observed range of wave phase speeds.

[28] Of particular importance for our DAWEX investigations are the measurements of the wave propagation headings which show an overwhelming preference for southward motion. Previous investigations of this nature at middle and low latitudes have also revealed significant anisotropy in wave propagation headings [e.g., *Taylor et al.*, 1993; *Medeiros et al.*, 2003; *Nakamura et al.*, 2003]. Possible causes of this anisotropy are: (1) nonuniformity in the geographic distribution of the wave sources, (2) critical layer filtering effects arising from background winds in the middle atmosphere, and (3) asymmetry in the source wave field due to strong wind shears in the upper troposphere [e.g., *Alexander et al.*, 2004]. Assuming the majority of the observed wave events were generated by convective forcing, comparison of their azimuthal wave distribution with the Japanese GMS satellite data, suggests two main regions of strong convection during this period; one due to localized thunderstorm activity in the Darwin area while the other is associated with intense storm activity over the Indonesian archipelago, at a much larger range. This latter storm activity is primarily associated with the Intertropical Convergence Zone (ITCZ). Recent airglow measurements from southern Indonesia by *Nakamura et al.* [2003] also suggest nonuniformity in storm activity as the cause of strong observed southward gravity wave propagation. The abundance of convective sources to the north of Katherine and Wyndham during the DAWEX campaign therefore

appears to play a major role in the observed propagation anisotropy.

[29] However, *Taylor et al.* [1993] have also shown how the background wind field in the stratosphere and lower mesosphere can significantly limit the upward flux of waves depending upon their phase speeds and headings. This condition, called critical layer filtering, arises when the background wind in the direction of motion of a wave becomes equal in magnitude to its observed phase speed [e.g., *Booker and Bretherton*, 1967; *Fritts*, 1978]. As the waves approach this condition they can be reflected or absorbed into the background medium thereby preventing them from reaching the MLT region. Figure 6 shows a composite plot of the zonal and meridional wind components as a function of altitude (up to 90 km), representative of the IOP 2 [*Hamilton et al.*, 2004]. In this figure, the UK Meteorological Office (UKMO) wind data from the ground up to the stratopause have been extended upward to the mesopause region using a wind climatology previously developed from the Upper Atmosphere Research Satellite (UARS) data [*Swinbank and Ortland*, 2003]. Atmospheric tidal effects, which are important above ∼60 km, were then incorporated using the Global Scale Wave Model (GSWM) predictions for this site and time of year [*Hagan et al.*, 1999]. The resultant model winds were then tuned to match coincident measurements of the mesospheric wind field obtained by MF radar from Katherine as part of the DAWEX IOP 2 observations. Figure 6 shows the nominal zonal and meridional wind field at 1430 UT (2230 LT at Wyndham). The zonal wind component remained relatively low (<20 m/s) throughout this altitude range suggesting only limited E-W critical layer filtering effects as the observed wave phase speeds were significantly larger (range 27–75 m/s) during this period. However, the meridional data are strongly influenced by the diurnal tide which exhibits significant growth in amplitude with height. The combination of zonal and meridional winds therefore indicates that critical layer filtering of the waves above about 70 km altitude would occur for observed phase speed of less than ∼50 m/s (northward motion) and less than ∼35 m/s (southward motion).

[30] Comparison with the velocity distribution of Figure 5 shows that the majority of the waves imaged in the OH emission (mean altitude ∼87 km) progressed southward with observed phase speeds of typically 40–60 m/s. As these waves are significantly faster than the nominal background winds they would be expected to propagate freely into the upper mesospheric region, which is fully consistent with our observations. In addition, two of the four northward moving wave events exhibited the largest observed phase speeds (>60 m/s), which is also consistent with the concept of stronger wind filtering effects for northward wave progression. (Note, as the wind field of Figure 6 is only a best estimate of its true value, it is only used here to provide general information on the expected wind filtering effects.)

[31] Finally, the limited observed westward wave progression may, in part, be explained by the modeling results of *Alexander et al.* [2004] that utilized radiosonde and boundary layer radar wind data recorded from the Tiwi Islands during the IOP 2 to model the generation of gravity waves in the vicinity of Darwin. Their results (which used
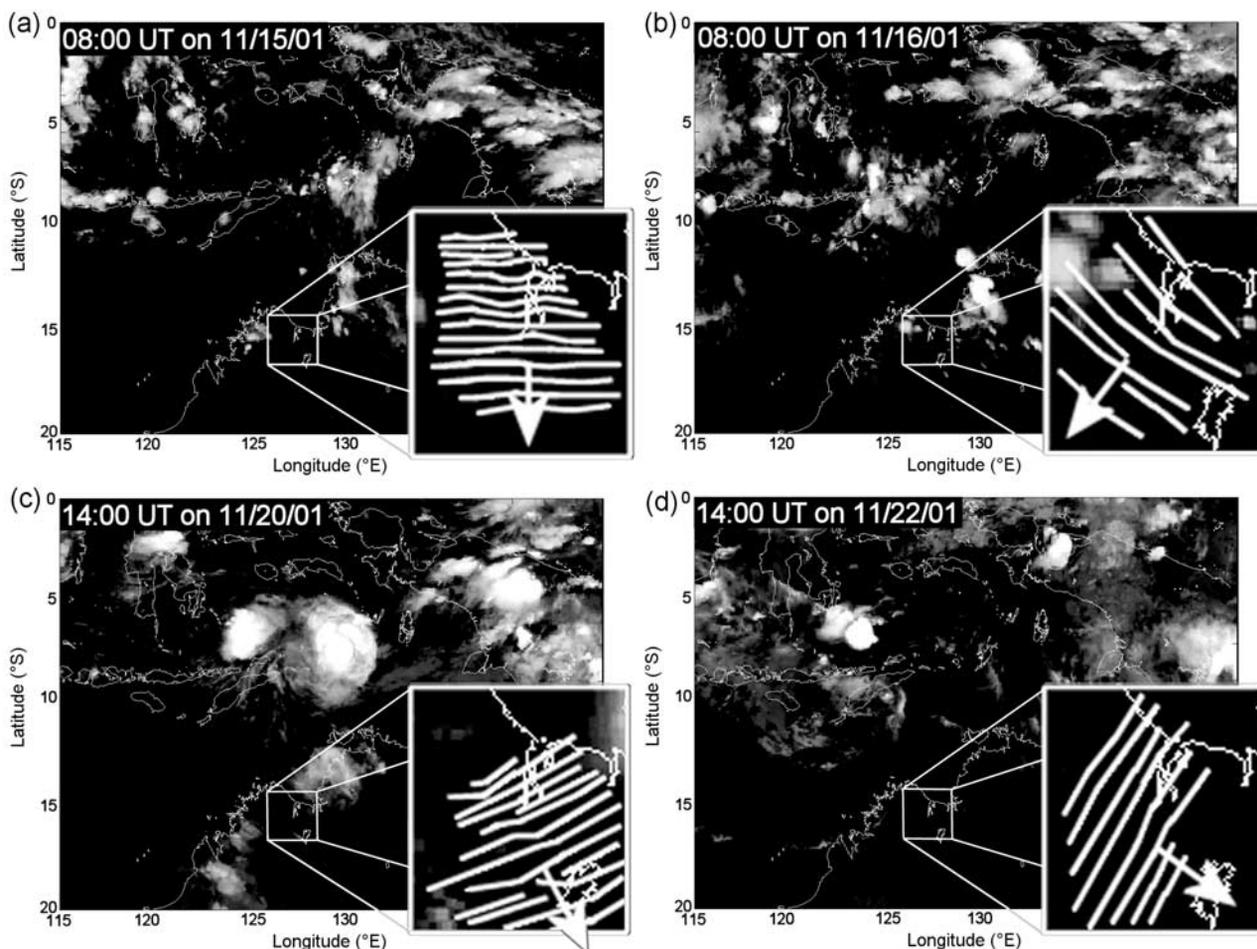
Figure 7. Examples of infrared satellite images showing convective activity (indicated by white cloud tops) over a 20° latitude by 30° longitude region encompassing northern Australia and southern Indonesia for four nights when prominent gravity waves were observed from Wyndham. In each case the OH wave patterns are plotted inside the expanded white box representing a 300 × 300 km square region. The white arrows indicate the observed direction of motion of each event. The ΔT indicates the time between the satellite image and the wave detection.

data from 17/18 November) show that most of the gravity wave energy at the 22 km height level (the model does not trace the energy transfer into the mesosphere), propagated toward the east (and north) with only limited energy toward the west. This asymmetry was caused by the presence of a significant wind shear in the upper troposphere on this occasion. In summary, our observed anisotropy in wave propagation headings during IOP 2 was most probably due to the dominant convective source regions lying mainly to the north of Wyndham and Katherine, compounded by wind filtering effects at the source altitude and within the middle atmosphere limiting the distribution of the lower observed phase speeds.

[32] To further investigate the dominant source regions, Figure 7 shows four of the most prominent wave events recorded in the OH emission from Wyndham during IOP 2. The data were first mapped onto the Earth's surface for an assumed altitude of 87 km (see section 3) and then their main features were traced to show their horizontal scale sizes, orientation, and coherence with their direction of motion indicated by an arrow. In each example, the wave

data are plotted inside an expanded box that represents a 300 × 300 km square region centered on Wyndham. These maps are shown superimposed on an infrared brightness temperature image from the GMS satellite which identifies regions of deep convective activity (strong white areas representing cold temperatures at high altitudes), as well as lower-altitude cloud cover (gray areas) over a 20° latitude range, encompassing northern Australia and southern Indonesia.

[33] Using the gravity wave dispersion relation for an ideal, stationary atmosphere [*Hines*, 1960], we estimate that the group velocity of a wave with mean values $\lambda_h = 30$ km, $v_h = 50$ m/s and $\tau \sim 10$ min (similar to those observed during the DAWEX campaign), would be about 35 m/s. However, in a real atmosphere background winds can significantly alter the time of flight of the waves which may also undergo reflection or absorption at a critical levels [e.g., *Taylor et al.*, 1993], or become ducted in the vicinity of the mesopause by strong temperature or wind gradients [e.g., *Isler et al.*, 1997; *Walterscheid et al.*, 1999]. Figure 6 shows that the background wind field was relatively low
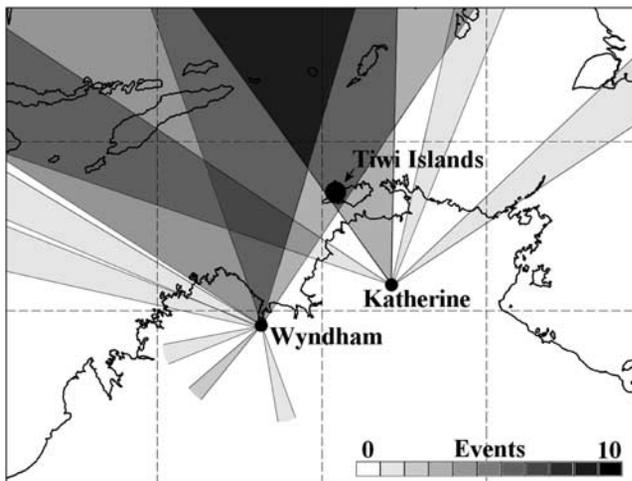
Figure 8. Plot showing the backward extension of the wave azimuths of Figure 5 to illustrate the main regions of overlap of the two data sets. (This plot is not to be confused with a true reverse ray tracing analysis.) The shaded areas identify the main azimuthal sectors from which the waves most likely originated. In each case the amount of shading represents the number of events observed within a given region. The dominant source regions appear to lie to the north and northwest of Australia.

(<20 m/s below ∼60 km) and a conservative estimate of the propagation time for waves generated in the Darwin area to reach the upper mesosphere over Katherine and Wyndham would be about 1–4 hours. The GMS satellite maps are available every three hours and, in each case, we have selected maps that occur within ∼1 to 4 hours of the observed onset of the wave events to show the best available information on the dominant prevailing convective activity.

[34] All four wave events plotted in Figure 7 exhibit a strong southward component of motion representative of the majority of the data set. Figure 7a shows a linear set of bands that was observed briefly (<20 min) on 15/16 November at 1048 UT, progressing almost due south prior to the onset of cloud. As discussed earlier in section 4, a near identical wave (event 2) with a similar propagation azimuth (175°N) was observed over 7 hours later, suggesting the possibility of a second source. In this example, the satellite data (0800 UT) show the convective activity at 2 hour 48 min prior to the wave event (no weather data are available at a shorter time interval). The satellite image reveals remnant high-altitude cloud to the NE over the Darwin/Tiwi Island area, following strong storm activity (including Hector) earlier in the day. However, the GMS imagery shows no obvious signs of any significant convective activity over the ocean to the north of Wyndham within several hundred kilometers, at this time and also earlier and later. A similar situation prevailed for Figures 7c and 7d which were recorded later in IOP 2 on 20/21 and 22/23 November. The satellite images are shown at 1400 UT in each case and the corresponding time differences were 1 hour 34 min for Figure 7c and 3 hour 15 min for Figure 7d. In both of these examples the OH waves progressed toward the ∼SE yet there is no evidence of local convection in the satellite

data toward the N-NW. However, the satellite data do show strong convective activity lying to the north over Indonesia but at a range of at least 800–1000 km.

[35] In contrast to these three examples, Figure 7b shows gravity wave progression toward the SSW, during the night of the 16/17 November, in good alignment with convection in the vicinity of Darwin. On this occasion, strong thunderstorm activity developed in this area during the course of the afternoon (Hector) and evening hours (squall line), as evident in the satellite data which was recorded 3 hour 18 min prior to the detection of the gravity wave event. On the following night (17/18 November), a similar situation also occurred with wave structures favorably oriented toward the Darwin area. A detailed description of these two southwestward wave events together with a ray tracing analysis is given in the work of M. J. Taylor et al. (manuscript in preparation, 2005). Here we wish to continue our discussion on the majority of the wave events observed during the premonsoon period which showed an overwhelming preference for wave progression toward approximately the SSE.

[36] The Wyndham and Katherine sites were selected to optimize our capability to discriminate between freely propagating waves, locally generated by regional sources over northern Australia, as compared with ducted gravity waves that can travel much larger horizontal distances from their source regions [e.g., *Isler et al.*, 1997]. In particular, the contribution of ducted waves from sources as far north as Indonesia may be significant. As a matter of fact, long-range ducting has been proposed to explain previous observations of short-period gravity waves over southern Australia by *Walterscheid et al.* [1999], and also during the DAWEX campaign by *Hecht et al.* [2004]. Figure 1 shows that Katherine lies to the ∼SSE of the Tiwi Islands, while Wyndham is located to the ∼SSW. Locally generated wave would therefore be expected to exhibit quite different propagation azimuths at these two sites whereas long-range waves would exhibit similar propagation azimuths at both sites.

[37] In Figure 8, we examine the possible source regions for the waves imaged from Katherine and Wyndham during the IOP 2. The data were taken from Tables 2 and 3. As a first step in this investigation, the azimuthal data have simply been extended backward to illustrate the main regions of overlap of the two data sets. This plot is not to be confused with a true reverse ray tracing analysis (which is beyond the scope of this study), but provides a first look at the data to help identify the primary source regions. In this plot, the Wyndham data have been divided into three adjacent sectors (corresponding to the dominant wave azimuths evident in Figure 5). The amount of shading represents the number of events within each sector. For example, the northward sector has 6 events whereas the adjacent (left) sector has 4 events and adjacent (right) sector, that encompasses the Tiwi Islands, has only 3 events. The figure suggests that the majority of the wave events originated from the NW and N sectors, which are well-removed from regional convection over the general Darwin area. In addition, the Katherine data indicate wave propagation over a broad sector that encompasses both the expected localized storm activity in the Darwin area as well as distant convective regions to the NNW. Other individual wave events are depicted as ±5° wide beam (which represents the uncertainty

in the azimuthal measurements). Together these two data sets suggest that a large majority of the wave events (>75%), observed during IOP 2, may have originated from source regions located to the N and NW of Australia, possibly as distant as the Indonesian Island chain.

[38] The detection of strong southward flow during the DAWEX campaign is in full agreement with the measurements of *Walterscheid et al.* [1999] who also observed marked southward motion "toward the summer pole," but from southern Australia during 1995–1996. In particular, their data showed a clear preference for meridional flow that was poleward in summer and mainly equatorward in winter. Importantly, their gravity wave measurements were made from Adelaide (34.4°S) in southern Australia and they attributed the summer southward flow to distant thunderstorm activity (over the northern coast of Australia), as there was very little convective activity over the arid interior of Australia. These are the very same sources that the DAWEX campaign was designed to investigate. To explain our overwhelming result for southward flow, we in turn have attributed it to wave sources located even further toward the equator (possibly over Indonesia). This intriguing result suggests that, under the right conditions, short-period gravity waves can propagate over vast horizontal distances (several thousand km), most probably via a thermal ducting mechanism as postulated by *Walterscheid et al.* [1999].

[39] Finally, in addition to the dominant southward wave progression, the Wyndham data also show four gravity wave events with a northward component of motion (see Figure 5a). Three events moved toward the ∼NE-NNE while the forth progressed toward the ∼NNW. No northward event was recorded at Katherine. The satellite data showed no sign of convection to the south of Wyndham on these occasions. *Hecht et al.* [2004] also observed some northward wave motions, during IOP 2, from their two camera sites at Adelaide (34.4°S) and Alice Springs (23.4°S). They reported three events; two occurred on 19 November (for which there are no Wyndham observations) and one on 16 November heading toward the ∼NE as observed from Alice Springs. This event persisted for over 5 hours (from 1200 to 1700 UT). At Wyndham, a similarly oriented wave (event 4) was also observed but it lasted for only ∼1 hour (from 1300 to 1400 UT). It is questionable that these two measurements are of the same wave event due to the large separation of the two observing sites which would require the wave pattern to extend over 1000 km in width. Hecht et al. also investigated the possibility that their northward moving events (for which they were also not able to identify a convective source), were generated in the southwestern part of Australia due to large amplitude ageostrophic flows which they postulated may be an alternative source of gravity waves to convection.

6. Summary

[40] The DAWEX campaign was conducted during the austral spring 2001 and provided an excellent opportunity to investigate short-period gravity wave characteristics and dynamics in the vicinity of expected intense thunderstorm convection over Northern Australia, close to Darwin and the Tiwi Islands. A network of instruments was deployed for this campaign which, together with detailed modeling

studies, was designed to provide a unique capability to study gravity waves generated by deep convection and their corresponding signatures at mesospheric heights. This paper focuses on the gravity waves observed in the OH nightglow emission during a 10-day period in November using two all-sky imagers located at Katherine 400 km to the ∼SSE of the Darwin area, and Wyndham 525 km to ∼SW. Although not discussed in detail, sever operational constraints prevailed during the campaign (e.g., extremely high temperatures, humidity and limited visibility), which often impaired the nominal performance of the imagers, yet these joint observations have yielded an important data set on the wave characteristics and their preferred propagation headings during this period. A total of 25 events were observed during IOP 2, which exhibited characteristics similar to short-period gravity wave measurements at other low-latitude sites, many of which had significantly higher phase speeds ∼50 m/s than those typically recorded at midlatitudes, resulting in relatively short observed periods ∼10 min.

[41] Surprisingly the majority of the wave events (84%) exhibited a strong SSE direction of motion suggesting dominant source regions to the NNW of Australia rather than originating from the general Darwin area. Observations of strong southward flow over central and southern Australia were also observed by *Hecht et al.* [2004] during the same period, and by *Suzuki et al.* [2004], whose measurements refer mainly to data obtained from Darwin during the summer months following the DAWEX campaign. On only two nights (16/17 and 17/18 November) gravity wave patterns were observed that aligned well with localized convection that occurred in the vicinity of the Tiwi Islands/Darwin area. These results suggest that strong regional convective activity over northern Australia was not the primary source of the observed OH wave structure during this period. (A detailed ray-tracing study of the wave data recorded on these two consecutive nights is the subject of a separate report.)

[42] An investigation of the observed anisotropy in the velocity distribution of the waves indicates a combination of three possible effects: nonuniformity in the source distribution, critical layer wind filtering in middle atmosphere, and strong wind shear at the source altitude restricting the resultant gravity wave field. Coincident satellite data show that the dominant convective source regions were located in the Darwin area and at a much larger range over Indonesia suggesting that the distribution of sources played a key role in the observed anisotropy in wave headings during this period. No significant storm activity was observed to the south over the Australian continent or over the ocean to the north of Wyndham. As the majority of the southward progressing wave events did not appear to originate from the general Darwin area, we are left with the possibility that they were generated by the copious convective sources at a much larger range over Indonesia. This result is in good agreement with the airglow measurements of *Walterscheid et al.* [1999] and *Hecht et al.* [2004], who also observed strong southward motion over central and southern Australia which they attributed to thermal ducting of the waves at the mesopause region as a mechanism for long range wave propagation. Our measurements from northern Australia also suggest that, under the right conditions, ducting

may be responsible for short-period gravity waves propagation over vast horizontal distances (several thousand km), well-removed from their source regions.

[43] Further coordinated measurement and modeling studies of convectively generated gravity waves are clearly needed to investigate their generation and propagation to mesospheric heights and their subsequent effects on the background medium. In particular, it is important to be able to distinguish between their motions (i.e., freely propagating or ducted) and to identify more clearly their dominant source regions.

References

Alexander, M. J., and J. R. Holton (1997), A model study of zonal forcing in the equatorial stratosphere by convectively induced gravity waves, *J. Atmos. Sci.*, *54*, 408.

Alexander, M. J., J. R. Holton, and D. Durran (1995), The gravity wave response above deep convection in squall line simulation, *J. Atmos. Sci.*, *52*, 2212.

Alexander, M. J., P. T. May, and J. H. Beres (2004), Gravity waves generated by convection in the Darwin area during the Darwin Area Wave Experiment, *J. Geophys. Res.*, *109*, D20S04, doi:10.1029/2004JD004729.

Baker, D. J., and A. T. Stair Jr. (1988), Rocket measurements of the altitude distributions of the hydroxyl airglow, *Phys. Scr.*, *37*, 611.

Beres, J. H., M. J. Alexander, and J. R. Holton (2004), A method of specifying the gravity wave spectrum above convection based on latent heating properties and background wind, *J. Atmos. Sci.*, *61*, 324.

Booker, J. R., and F. P. Bretherton (1967), The critical layer for internal gravity wave in a shear flow, *J. Fluid Mech.*, *27*(3), 513.

Broadfoot, A. L., and K. R. Kendall (1968), The airglow spectrum, 3100–10,000 A, *J. Geophys. Res.*, *73*, 426.

Carbone, R. E., T. D. Keenan, J. M. Hacker, and J. W. Wilson (2000), Tropical island convection in the absence of significant topography. Part I: Sea breeze and early convection, *Mon. Weather Rev.*, *128*, 3459.

Coble, M. R., G. C. Papen, and C. S. Gardner (1998), Computing two-dimensional unambiguous horizontal wavenumber spectra from OH airglow images, *IEEE Trans. Geosci. Remote Sens.*, *36*, 2.

Ejiri, M. K., K. Shiokawa, T. Ogawa, K. Igarashi, T. Nakamura, and T. Tsuda (2003), Statistical study of short-period gravity waves in OH and OI nightglow images at two separated sites, *J. Geophys. Res.*, *108*(D21), 4679, doi:10.1029/2002JD002795.

Fritts, D. C. (1978), The nonlinear gravity wave-critical level interaction, *J. Atmos. Sci.*, *35*, 397.

Fritts, D. C., and M. J. Alexander (2003), Gravity wave dynamics and effects in the middle atmosphere, *Rev. Geophys.*, *41*(1), 1003, doi:10.1029/2001RG000106.

Fritts, D. C., J. R. Isler, G. E. Thomas, and Ø. Andreassen (1993), Wave breaking signatures in noctilucent clouds, *Geophys. Res. Lett.*, *20*, 2039.

Fritts, D. C., J. R. Isler, and Ø. Andreassen (1994), Gravity wave breaking in two and three dimensions: 2. Three-dimensional evolution and instability structure, *J. Geophys. Res.*, *99*, 8109.

Garcia, F. J., M. J. Taylor, and M. C. Kelley (1997), Two-dimensional spectral analysis of mesospheric airglow image data, *Appl. Opt.*, *36*(29), 7374.

Garcia, R. R., and S. Solomon (1985), The effects of breaking gravity waves on the dynamics and chemical composition of the mesosphere and lower thermosphere, *J. Geophys., Res.*, *90*, 3850.

Gardner, C. S., M. Coble, G. C. Papen, and G. R. Swenson (1996), Observations of the unambiguous 2-dimensional horizontal wave number spectrum of OH intensity perturbations, *Geophys. Res. Lett.*, *23*, 3739.

Hagan, M. E., M. D. Burrage, J. M. Forbes, J. Hackney, W. J. Randel, and X. Zhang (1999), GSWM-98: Results for migrating solar tides, *J. Geophys. Res.*, *104*, 6813.

Hamilton, K. (1996), Comprehensive meteorological modeling of the middle atmosphere: Tutorial review, *J. Atmos. Terr. Phys.*, *58*, 1591.

Hamilton, K., and R. A. Vincent (2000), Experiment will examine gravity waves in the middle atmosphere, *Eos Trans. AGU*, *81*(44), 517.

Hamilton, K., R. A. Vincent, and P. T. May (2004), Darwin Area Wave Experiment (DAWEX) field campaign to study gravity wave generation and propagation, *J. Geophys. Res.*, *109*, D20S01, doi:10.1029/2003JD004393.

Hecht, J. H. (2004), Instability layers and airglow imaging, *Rev. Geophys.*, *42*, RG1001, doi:10.1029/2003RG000131.

Hecht, J. H., R. L. Walterscheid, J. Woithe, L. Campbell, R. A. Vincent, and I. M. Reid (1997), Trends of airglow imager observations near Adelaide, Australia, *Geophys. Res. Lett.*, *24*, 587.

Hecht, J. H., R. L. Walterscheid, and R. A. Vincent (2001), Airglow observations of dynamical (wind shear-induced) instabilities over Adelaide, Australia, associated with atmospheric gravity waves, *J. Geophys. Res.*, *106*, 28,189.

Hecht, J. H., S. Kovalam, P. T. May, G. Mills, R. A. Vincent, R. L. Walterscheid, and J. Woithe (2004), Airglow imager observations of atmospheric gravity waves at Alice Springs and Adelaide, Australia during the Darwin Area Wave Experiment (DAWEX), *J. Geophys. Res.*, *109*, D20S05, doi:10.1029/2004JD004697.

Hines, C. O. (1960), Internal atmospheric gravity waves, *Can. J. Phys.*, *38*, 1441.

Holton, J. R. (1983), The influence of gravity wave breaking on the circulation of the middle atmosphere, *J. Atmos. Sci.*, *40*, 2497.

Holton, J. R., and M. J. Alexander (1999), Gravity waves in the mesosphere generated by tropospheric convection, *Tellus*, *51*, 45.

Holton, J. R., J. H. Beres, and X. L. Zhou (2002), On the vertical scale of gravity waves excited by localized thermal forcing, *J. Atmos. Sci.*, *59*(12), 2019.

Horinouchi, T., T. Nakamura, and J. Kosaka (2002), Convectively generated mesoscale gravity waves simulated throughout the middle atmosphere, *Geophys. Res. Lett.*, *29*(21), 2007, doi:10.1029/2002GL016069.

Isler, J. R., M. J. Taylor, and D. C. Fritts (1997), Observational evidence of wave ducting and evanescence in the mesosphere, *J. Geophys. Res.*, *102*, 26,301.

Keenan, T. D., and R. E. Carbone (1992), A preliminary morphology of precipitation systems in tropical northern Australia, *Q. J. R. Meteorol. Soc.*, *118*, 283.

Lindzen, R. S. (1981), Turbulence and stress owing to gravity wave and tidal breakdown, *J. Geophys. Res.*, *86*, 9707.

Medeiros, A. F., M. J. Taylor, H. Takahashi, P. P. Batista, and D. Gobbi (2003), An investigation of gravity wave activity in the low-latitude upper mesosphere: Propagation direction and wind filtering, *J. Geophys. Res.*, *108*(D14), 4411, doi:10.1029/2002JD002593.

Medeiros, A. F., R. A. Buriti, E. A. Machado, M. J. Taylor, H. Takahashi, P. P. Batista, and D. Gobbi (2004), Comparison of gravity wave activity observed by airglow imaging from two different latitudes in Brazil, *J. Atmos. Sol. Terr. Phys.*, *66*, 647.

Moreels, G., and M. Herse (1977), Photographic evidence of waves around the 85 km-level, *Planet. Space Sci.*, *25*, 265.

Nakamura, T., A. Higashikawa, T. Tsuda, and Y. Matsushita (1999), Seasonal variations of gravity wave structures in OH airglow with a CCD imager at Shigaraki, *Earth Planets Space*, *51*, 897.

Nakamura, T., T. Aono, T. Tsuda, A. G. Admiranto, E. Achmad, and Suranto (2003), Mesospheric gravity waves over a tropical convective region observed by OH airglow imaging in Indonesia, *Geophys. Res. Lett.*, *30*(17), 1882, doi:10.1029/2003GL017619.

Pautet, D., and G. Moreels (2002), Ground-based satellite-type images of the upper-atmosphere emissive layer, *Appl. Opt.*, *41*(5), 823.

Peterson, A. W. (1979), Airglow events visible to the naked eye, *Appl. Opt.*, *18*, 3390.

Rezaul, H., and G. R. Swenson (1999), Extraction of motion parameters of gravity-wave structures from all-sky OH image sequences, *Appl. Opt.*, *38*, 4433.

Smith, S. M., M. Mendillo, J. Baumgardner, and R. R. Clark (2000), Mesospheric gravity wave imaging at a subauroral site: First results from Millstone Hill, *J. Geophys. Res.*, *105*, 27,119.

Suzuki, S., K. Shiokawa, Y. Otsuka, T. Ogawa, and P. Wilkinson (2004), Statistical characteristics of gravity waves observed by an all-sky imager at Darwin, Australia, *J. Geophys. Res.*, *109*, D20S07, doi:10.1029/2003JD004336.

Swenson, G. R., and C. S. Gardner (1998), Analytical models for the responses of the mesospheric Na and OH* layers to atmospheric gravity waves, *J. Geophys. Res.*, *103*, 6271.

Swenson, G. R., and S. B. Mende (1994), OH emissions and gravity waves (including a breaking wave) in all-sky imagery from Bear Lake, Utah, *Geophys. Res. Lett.*, *21*, 2239.

Swenson, G. R., M. J. Taylor, P. J. Espy, C. S. Gardner, and X. Tao (1995), ALOHA-93 measurements of intrinsic AGW characteristics using airborne airglow imager and ground based Na wind/temperature lidar, *Geophys. Res. Lett.*, *22*, 2841.

Swenson, G. R., R. Haque, W. Yang, and C. S. Gardner (1999), Momentum and energy fluxes of monochromatic gravity waves observed by an OH imager at Starfire Optical Range, NM, *J. Geophys. Res.*, *104*, 6067.

Swinbank, R., and D. A. Ortland (2003), Compilation of wind data for the Upper Atmosphere Research Satellite (UARS) Reference Atmosphere Project, *J. Geophys. Res.*, *108*(D19), 4615, doi:10.1029/2002JD003135.

Taylor, M. J., and F. J. Garcia (1995), A two-dimensional spectral analysis of short period gravity waves imaged in the OI (557.7 nm) and near-infrared OH nightglow emissions over Arecibo, Puerto Rico, *Geophys. Res. Lett.*, *22*, 2473.

Taylor, M. J., and M. A. Hapgood (1990), On the origin of ripple-type wave structure in the OH nightglow emission, *Planet. Space Sci.*, *38*, 1421.

Taylor, M. J., and K. Henriksen (1989), *Electromagnetic Coupling in the Polar Clefts and Caps*, edited by P. E. Sandholdt and A. Egeland, Springer, New York.

Taylor, M. J., and M. J. Hill (1991), Near infrared imaging of hydroxyl wave structure over an ocean site at low latitudes, *Geophys. Res. Lett.*, *18*, 1333.

Taylor, M. J., E. H. Ryan, T. F. Tuan, and R. Edwards (1993), Evidence of preferential directions for gravity wave propagation due to wind filtering on the middle atmosphere, *J. Geophys. Res.*, *98*, 6047.

Taylor, M. J., M. B. Bishop, and V. Taylor (1995a), All-sky measurements of short period waves imaged in the OI (557.7 nm), Na (589.2 nm) and near infrared OH and O_2 (0,1) nightglow emissions during the ALOHA-93 campaign, *Geophys. Res. Lett.*, *22*, 2833.

Taylor, M. J., V. Taylor, and R. Edwards (1995b), An investigation of thunderstorms as a source of short period mesospheric gravity waves, in *The Upper Mesosphere and Lower Thermosphere: A Review of Experiment and Theory, Geophys. Monogr. Ser.*, vol. 87, edited by R. M. Johnson and T. L. Killeen, p. 177, AGU, Washington, D. C.

Taylor, M. J., W. R. Pendleton Jr., S. Clark, H. Takahashi, D. Gobbi, and R. A. Goldberg (1997), Image measurements of short-period gravity waves at equatorial latitudes, *J. Geophys. Res.*, *102*, 26,283.

Tsuda, T., M. V. Ratnam, P. T. May, M. J. Alexander, R. A. Vincent, and A. MacKinnon (2004), Characteristics of gravity waves with short vertical wavelengths observed with radiosonde and GPS occultation during the Darwin Area Wave Experiment (DAWEX), *J. Geophys. Res.*, *109*, D20S03, doi:10.1029/2004JD004946.

Vincent, R. A., A. MacKinnon, I. M. Reid, and M. J. Alexander (2004), VHF profiler observations of winds and waves in the troposphere during the Darwin Area Wave Experiment (DAWEX), *J. Geophys. Res.*, *109*, D20S02, doi:10.1029/2004JD004714.

Walterscheid, R. L., J. H. Hecht, R. A. Vincent, I. M. Reid, J. Woithe, and M. P. Hickey (1999), Analysis and interpretation of airglow and radar observations of quasi-monochromatic gravity waves in the upper mesosphere and lower thermosphere over Adelaide, Australia (35 S, 138 E), *J. Atmos. Sol. Terr. Phys.*, *61*, 461.

Wu, Q., and T. L. Killeen (1996), Seasonal dependence of mesospheric gravity waves (<100 km) at Peach Mountain Observatory, Michigan, *Geophys. Res. Lett.*, *23*, 2211–2214.

———————————

A. Z. Liu and G. R. Swenson, Department of Electrical and Computer Engineering, University of Illinois, Urbana, IL 61082, USA.

P.-D. Pautet and M. J. Taylor, Center for Atmospheric and Space Sciences, Utah State University, Logan, UT 84322, USA. (pautet@cc. usu.edu)